Core-level spectroscopy study of rare-earth metal/W(110) interface formation

# Core-level spectroscopy study of rare-earth metal/W(110) interface formation

N P Tucker†, R I R Blyth†§, R G White†‡||, M H Lee†, C Searle† and S D Barrett†‡

† Surface Science Research Centre, University of Liverpool, PO Box 147, Liverpool L69 3BX, UK
‡ Department of Physics, University of Liverpool, PO Box 147, Liverpool L69 3BX, UK

**Abstract.** The electronic structure of rare-earth metal/W(110) interfaces during the initial stages of deposition has been investigated using core-level shift spectroscopy. Three rare-earth metals (Gd, Y and Yb) have been grown on a W(110) substrate. Shifts in the W $4f_{7/2}$ core level peaks of >300 meV have been confirmed for the clean W(110) surface. On completion of each interface a bulk feature and only one shifted peak is observed which supports evidence that no alloying occurs. At submonolayer coverages an additional feature is seen at higher kinetic energies which is attributed to emission from W atoms under various $(n \times 2)$ adsorbate structures.

## 1. Introduction

Research into rare-earth metals grown on various refractory-metal substrates has been active for over a decade. The most common substrate employed is the close-packed W(110) face, which provides epitaxial growth with no alloying. Of the rare earths, Gd has received by far the most attention, due mainly to its novel surface magnetic properties [1]. While the majority of the published work on rare earths has focused on properties of thick films, this paper presents a study of the initial stages of growth and is concerned with the interface formation that occurs during the deposition of the first few layers of adsorbate.

A surface structure determination using quantitative low energy electron diffraction (LEED) undertaken by Giergiel *et al* [2] of a 400 Å thick Gd film grown on W(110) gave excellent agreement with an earlier study of a Gd(0001) single crystal [3], hence showing that thick films grow as the (0001) face. However in the initial stages of growth there is a lattice mismatch between the W(110) and rare-earth(0001) faces of ∼15%, so the interfaces are unlikely to be truly epitaxial. The resulting strain induced in Gd layers is only relieved for films >100 Å thick [4]. Kolaczkiewicz and Bauer [5] studied the submonolayer growth of Gd on W(110) using qualitative LEED and reported a series of $(n \times 2)$ structures in the sequence $(10 \times 2)$, $(7 \times 2)$, $(6 \times 2)$ and $(5 \times 2)$, before observing a $c(5 \times 3)$ pattern with hexagonal structures following for coverages >0.6 monolayers (ML). It is reasonable to assume that similar structures will exist for Y and Yb growth on W(110).

§ Present address: Institut für Experimentalphysik, Karl Franzens Universität Graz, Universitätsplatz 5, A-8010 Graz, Austria.
|| Present address: VG Scientific, The Birches Industrial Estate, Imberhorne Lane, East Grinstead, West Sussex RH19 1UB, UK.

Changes in the environment of atoms manifests itself as a shift in the binding energies of core-level peaks of the atoms—a core-level shift (CLS). These environmental changes can be chemical, electronic or structural in nature. For instance the electronic and structural changes in the environment of atoms at a surface causes a shift in their core-level photoemission peaks with respect to the energy position of the bulk-related peak. This is known as the surface core-level shift (SCLS). The 4f levels of W provided the first experimental evidence of the SCLS [6]—this was due to the large surface shift and narrow intrinsic linewidth of these features. Since then many studies have been performed of the CLS of W surfaces including clean (110) [7], stepped (110) [8], W(001) [9], WC(0001) [10] and adsorption of O [11], H [12] and S [13] on W(001).

Thus CLS spectroscopy is a useful tool in elucidating changes in the environment of the topmost W atoms as an adsorbate is deposited. The altered environment of W atoms initially at the clean surface, caused by the deposition of the rare-earth metal, leads to a modification in the CLS observed for the W 4f levels. However, this is expected to be small—so excellent experimental resolution is required to measure these shifts.

There have been previous CLS studies of rare earths grown on W(110), but these have focused on the smaller shift present in rare-earth 4f levels of a thick film [14–16]. White *et al* [17] have published the only CLS study of the initial stages of growth of a rare-earth metal (Gd on W(110)). In this paper we present new Gd/W(110) data taken with increased resolution and fitted with Doniach–Sunjic lineshapes [18] convoluted with Gaussians, rather than the Voigt lineshape approximation employed in the earlier study [17]. New data for Y and Yb grown on W(110) are presented. Yttrium is similar to Gd, both structurally and electronically. It shares the hcp crystal structure and Y films also exhibit a hexagonal LEED pattern corresponding to the (0001) face. Electronically it has an analogous trivalent valence configuration ($4d^15s^2$, with Gd being $5d^16s^2$), although it has no 4f electrons. Yb is significantly different—its bulk crystal structure is fcc and a hexagonal LEED pattern is observed from thin films, corresponding to two domains of the threefold symmetric (111) face. Its valence configuration is $(5d6s)^2$ making it divalent, and it possesses a full 4f shell.

## 2. Experimental details

The measurements were taken on the Surface Science Research Centre's VUV beamline 4.1 [19] at the Synchrotron Radiation Source, Daresbury Laboratory, UK. The Gd data set was collected on a Scienta SES200 hemispherical analyser, which gave a total energy resolution (photon bandwidth and analyser resolution) of 90 meV at $h\nu = 70$ eV. A Vacuum Science Workshop HA54 analyser was used to collect the Y and Yb data sets, giving a total energy resolution of 190 meV at $h\nu = 70$ eV. The chamber was equipped with Omicron 4-grid LEED optics, which were also used in RFA mode to collect Auger spectra.

The W(110) sample was cut from a commercially obtained boule with a purity >99.99%, and subsequently polished to within $1°$ of the (110) face. *In situ* cleaning of the sample was achieved by backfilling the chamber with $1 \times 10^{-6}$ mbar $O_2$ and heating the sample to 1500 K for 60 minutes to remove carbon, followed by periodic flashing to 2300 K. Surface cleanliness was monitored using LEED, Auger electron spectroscopy and by monitoring the photoemission from both the valence band and the W 4f core-level shift which is known to be sensitive to contamination [7].

The Gd was evaporated from an Omicron EFM4 electron-beam evaporator, the Y was evaporated from a water-cooled, tungsten wire basket evaporator [20] and the Yb was evaporated from a WA Technology Knudsen cell. Each evaporator was extensively outgassed prior to deposition. An evaporation temperature of $\sim$1400 K was used for the

Gd and Y, whereas Yb was grown at ∼800 K due to its higher vapour pressure at a given temperature. The chamber base pressure was $<1 \times 10^{-10}$ mbar for each of the three experiments, and remained $<2 \times 10^{-10}$ mbar during evaporation. The substrate was held at room temperature during growth as this is believed to promote layer-by-layer growth [5]. The deposition rate was estimated from the attenuation of the W 4f signal with deposition, and from monitoring the photoemission signal from the overlayer during growth [21].

Spectra were collected using a photon energy of 70 eV to ensure high surface sensitivity. The Y and Yb data sets were collected using an incidence angle of 5° and emission angle of 35° (all angles relative to surface normal), which allowed spectra to be collected during deposition. As the Scienta analyser was fixed in position this experimental geometry could not be used. Accordingly the Gd data set was collected by growing the film and then rotating the sample to normal emission geometry, with an angle of incidence of 30°. Clean W spectra taken at the 35° emission angle showed only slight differences in peak intensity, and not position, when compared to the normal emission spectra. Thus using a normal emission angle had no effect on the CLS measured but gave the advantage of an improved count rate.

## 3. Results and discussion

Figure 1 shows the flux-normalized spectra taken for Gd, Y and Yb growth. It can be seen in all three data sets that the intensity of the bulk peak B decreases with deposition time, and is slightly shifted towards a higher kinetic energy (by 80 meV for Gd and Y, and by 20 meV for Yb). The surface peak S is rapidly attenuated as the clean W surface becomes covered with the rare-earth adsorbate.
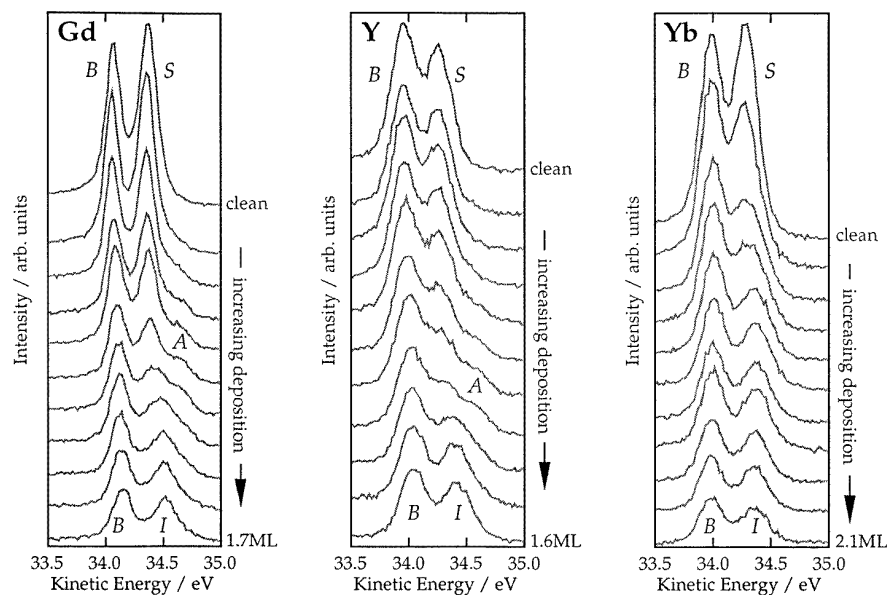


**Figure 1.** The W $4f_{7/2}$ photoemission signal as a function of rare-earth deposition for Gd, Y and Yb. The spectra were collected using a photon energy of $h\nu = 70$ eV with a 30° incidence angle and 0° emission angle Gd, and 5° incidence angle and 35° emission angle for Y and Yb (relative to surface normal).

For Gd and Y a peak, labelled A, clearly develops with deposition at a higher kinetic energy than either B or S. As deposition continues this feature then becomes less intense and finally disappears. This peak is not obvious in the Yb data set.

In the final spectra for each of the rare earths there are only two peaks present, the bulk peak B and another peak I, at a kinetic energy between peaks S and A. As the deposition of the films continues no further peaks are observed, but B and I are further attenuated as expected. Hence peak I can be associated with emission from W atoms at the completed rare-earth/W interface.

As peak A appears before I is seen, it would appear it is derived from emission from W atoms beneath the various submonolayer island structures reported by Kolaczkiewicz and Bauer [5]. This designation is further supported by the fact peak A is first seen when a contribution from the surface peak is present.

Four of the Gd spectra from figure 1 are plotted in figure 2. Spectrum (a) corresponds to emission from the clean W(110) surface. Spectra (b)–(d) correspond to continuing deposition of Gd, with the estimated deposition shown on the figure.
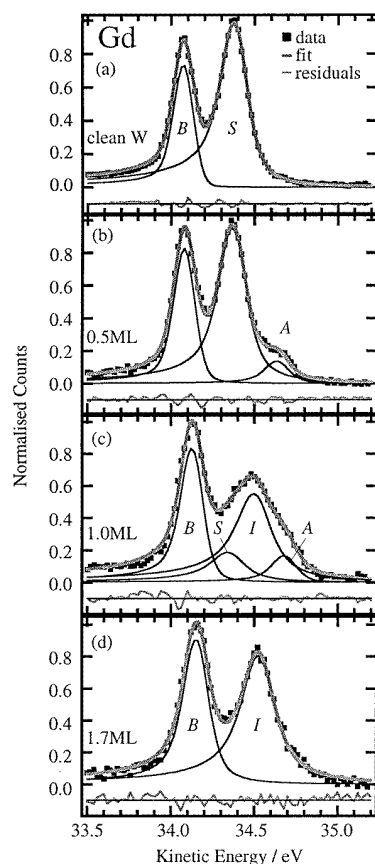


**Figure 2.** Four spectra from figure 1 corresponding to the clean W spectrum (a) and estimated coverages of (b) 0.5 ML, (c) 1.0 ML and (d) 1.7 ML of Gd. The spectra have been normalized to the bulk peak. Peaks corresponding to the bulk (B), surface (S), submonolayer components (A) and interface (I) have been fitted using Doniach–Sunjic curves convoluted with Gaussian lineshapes.

These estimates were obtained from three sources. Firstly the attenuation of the bulk peak B was used to obtain the coverage. A mean free path (or, more accurately, an attenuation length) of 2 ML was assumed for 34 eV kinetic energy electrons through the Gd [14]. The distinction between the mean free path and the attenuation length should be noted. Using the mean free path gives an overestimate of the coverage as it does not take account of elastic scattering within the sample—hence the characteristic attenuation length should be used [22]. Also, the use of the attenuation of bulk features to estimate coverage can give misleading results in the regime of very thin films. Discrepancies can be caused by localized atomic-like excitations and also surface-plasmon excitations at the substrate–overlayer and overlayer–vacuum interfaces [23]. Furthermore, shadowing effects caused by surface roughening may cause a non-exponential intensity variation [23]. Hence, the results obtained using this method were treated as a guide and not as a definitive coverage. Secondly, the Omicron evaporator had been calibrated using a timescan of the Gd 4f photoemission signal taken as a film was grown at the same flux. This gives an indication of the time taken for the completion of each monolayer of Gd [21]. Thirdly, the interpretation of the data offered indicates the coverages associated with the components present in any one spectrum. These coverages can then be interpolated for the other spectra in the data set.

Figures 3 and 4 show spectra taken from figure 1 for the growth of Y and Yb respectively. In both cases the top spectrum (a) corresponds to the clean W(110) surface, with the estimated deposition shown for each of the other spectra. This was derived from the attenuation of the bulk peak, and from the interpretation of the data as indicated above.

The data shown in figures 2–4 have been normalized to the bulk peak intensity and have subsequently been fitted using a standard photoemission lineshape. This lineshape is a convolution of the asymmetric Doniach–Sunjic function [18] (to model the natural lineshape) and a Gaussian (to model the experimental broadening). As they have the best statistics, the clean W spectra were used to determine the width of the Gaussian peak for each data set. This parameter is expected to remain the same throughout the data set, and so was fixed for each peak during the subsequent fits. The fitted peaks are shown in the figures, along with the residuals which give an indication of the quality of the fit. It can be seen that the residuals only show variations due to experimental noise; each fit returned an excellent chi-square value. Core level shifts obtained for the clean W samples are shown in table 1. They compare favourably to the values reported by Riffe *et al* [7, 8] for a clean W(110) surface.

**Table 1.** Core-level shifts of peaks S, A and I in the Gd, Y and Yb data sets.

|     | S (meV)     | A (meV)      | I (meV)     |
| --- | ----------- | ------------ | ----------- |
| Gd  | $308 \pm 3$ | $555 \pm 10$ | $375 \pm 5$ |
| Y   | $303 \pm 5$ | $575 \pm 15$ | $380 \pm 5$ |
| Yb  | $302 \pm 5$ | $425 \pm 30$ | $370 \pm 5$ |

Fitting spectra 2(d)–4(d) yielded the CLS of the peak corresponding to emission from W atoms at the buried W/rare-earth interface. It can be seen from table 1 that in all cases this CLS is greater than the SCLS by at least 65 meV. The values obtained for each rare-earth metal are within a range of 10 meV, and are consistent within the experimental error. A
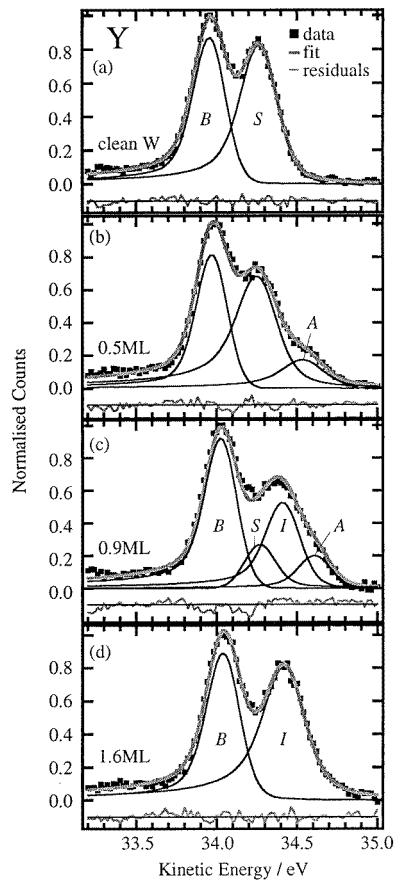
**Figure 3.** Four spectra from figure 1 corresponding to the clean W spectrum (a) and estimated coverages of (b) 0.5 ML, (c) 0.9 ML and (d) 1.6 ML of Y. Normalization and peak fitting as in figure 2.

fit with three peaks was also performed to ensure there were only two peaks present, and that formation of the interface was complete. The fit returned a near-zero intensity for the third peak, hence showing that only two peaks are present. The results imply the formation of a well ordered isotropic interface with no alloying. The evidence for a lack of alloying is further supported by the relatively small difference in CLS for the surface and interface peaks. If alloying had occurred a much larger range of core-level shifts would have been observed.

In fitting spectrum (b) in each data set, corresponding to a submonolayer coverage, the positions of the three peaks were left free. The data indicate that the SCLS decreases with coverage; this shift to a lower kinetic energy is observed more clearly for oxygen dosing of W(110) [9, 24].

Oxygen contamination from residual chamber gases can be ruled out as the cause of the shift observed in this study as the valence band spectra of each of the films was checked on completion of growth. Each spectrum was collected using $h\nu = 33$ eV photons, where emission from the O 2p level is easily recognized at around 5.6 eV binding energy [25]. Figure 5 shows the spectrum collected from the Y thin film on completion of growth (3 ML). By comparing the relative intensities of the O peak and the rare-earth surface state with those in the spectra taken by Zhang *et al* [25] from oxygen-dosed Gd thin films, it can be inferred that much less than 0.1 L of oxygen was deposited with the films.
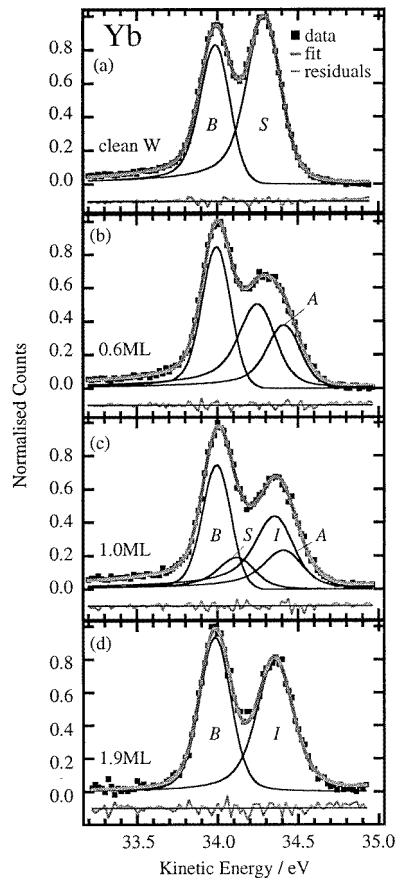
**Figure 4.** Four spectra from figure 1 corresponding to the clean W spectrum (a) and estimated coverages of (b) 0.6 ML, (c) 1.0 ML and (d) 1.9 ML of Yb. Normalization and peak fitting as in figure 2.

The apparent shift of the surface peak in oxygen-dosed W(110) has been interpreted as being due to its attenuation along with the appearance of another peak at a slightly lower kinetic energy [9]. However, the improved resolution of this study would show the presence of an additional peak as a broadening of the surface peak, which is not observed. Indeed the widths of S returned for the first three spectra of the Gd data set (which is the best resolved) differ by less than 10% which is less than the increase observed for the bulk peak. Furthermore, for spectrum (b) in each set both Gd and Y returned SCLS of 290 meV, while Yb returned a value of 260 meV, further vindicating the similar coverage assigned to the Gd and Y spectra and the increased coverage assigned to the Yb spectra.

In addition, spectra 2(b)–4(b) were also fitted with four peaks to ensure there was no contribution from peak I at those points. The Yb spectrum was also fitted with only two peaks as it not obvious from the raw data that a third peak is present. This resulted in an unsatisfactory fit of a higher chi square value, with the width of peak S being greatly increased and the residuals indicating missing weight from the high kinetic energy side of S.

Table 1 shows the CLS obtained for peak A. These values clearly vary over a greater range than experimental error would account for. The values returned for Gd and Y are consistent within experimental error, with Yb returning a considerably lower shift. As this peak arises from emission from W atoms under the submonolayer ($n \times 2$) structures,
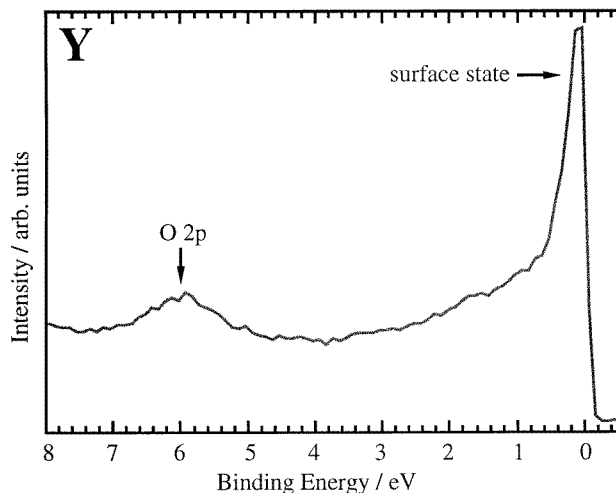
**Figure 5.** Valence band photoemission spectra from the Y film corresponding to the spectra in figure 3. The thickness of the film is 3 ML, with $h\nu = 33$ eV, 5° incidence angle and 35° emission angle.

it is likely that this peak has many individual contributions, each arising from W atoms with differing numbers of Gd neighbours. The number of near neighbours and their radial distribution will affect the charge transfer to a W atom, and hence slightly alter its CLS. The natural linewidth of these contributions when compared to their small relative shifts makes separation of them impossible, as a consequence the combined emission has been represented by a single peak in these fits.

Spectrum (c) in each set corresponds to around 1 ML of rare-earth metal deposition. In this thickness regime, peaks would be expected to be observed for emission from the bulk, from areas of clean W, from areas under smaller Gd islands and from under interfacial areas buried under larger islands. If the model proposed is correct, peaks B, S, A and I could be fitted to the spectra using the parameters already determined. The spectra have been fitted keeping the CLS of peaks A and I constant; S has been allowed to vary and in fact is found to move to a lower kinetic energy as is expected. The intensity of each peak was allowed to vary and the Gaussian width was fixed as before. Using these restraints good fits are obtained as can be seen from the figures. Each spectra was also fitted with three peaks as a check. In each case significantly better results were obtained for the fit with four peaks.

As can be seen from figures 2–4 the width of peak I is greater than peaks B and S. The narrow peaks B result from emission from atoms in a well ordered lattice, each with identical positions (lattice defects such as dislocations would have some influence, but this is not observed in our data). The increased width of peaks A indicates that they consist of individual contributions with a narrow range of CLS. A recent STM study revealed that the base monolayer of a Gd film on W(110) has a (7 × 14) periodicity with respect to the W substrate [26]. This will hence lead to W atoms at the interface with slightly differing coordinations to the Gd atoms, each with a slightly different CLS. By examining the widths of the peaks returned from the fits for several spectra no general trend for the increase in width for peak I was found between the different rare-earth metals. Hence there is no indication in this data of differing periodicities in the overlayer.

Final-state screening effects, caused by the valence electrons relaxing and screening the localized positive charge resulting from the emission of the photoelectron, influence the SCLS. Possible differences in screening for bulk and surface atoms give rise to an additional final-state contribution to the SCLS [34]. However, this contribution is fixed for an elemental clean surface. Subsequent deposition of an adsorbate and the resulting charge transfer will alter the valence electron distributions of W atoms at the developing interface and hence their screening effect. Any role played by these final-state screening effects will be very difficult to isolate, and for the purposes of this discussion they are included with the comments regarding the change in CLS caused by charge transfer in general.

The alkali and alkali-earth metals' electropositive nature leads to a marked decrease in work function upon deposition onto W substrates. This has been attributed to charge transfer from the valence band of the adsorbate to the substrate [27–30]. This mechanism is also consistent with the sign of the shifts observed for the rare earths in this study, i.e. electron donation from the adsorbate to the substrate giving shifts to a higher kinetic energy. Electron energy loss spectroscopy (EELS) should show this charge transfer for low coverages, and indeed this experiment has been conducted on Gd/W(110) [31]. The results indicated that there is no charge transfer from the 6s levels to the substrate as no losses due to the 5p–6s excitation were observed. It was suggested that the adsorbate layer was not ionic but in fact consisted of highly polarized atoms. These results do not rule out the possibility of charge transfer from the valence 5d shell. However a later experiment using Auger electron studies over the 4d ionization edge [32] showed that the valence band plays no part in the recombination process below a minimum coverage, suggesting that the adsorbate atoms are in fact ionized. Thus, the mechanisms underlying any charge transfer from adsorbate to substrate are unclear.

The CLSs observed upon completion of the interface are very similar with each of the three rare earths being slightly electropositive with respect to the surface W atoms. In particular, the similarity between Y and the other two rare earths suggests that the 4f levels do not play a significant part in the charge transfer. The reduction in the CLS observed for the submonolayer components for Yb most likely relates to a structural change as opposed to its differences in electronic configuration. As the Yb was evaporated at a much lower temperature, its mobility on initial contact with the W substrate would be greatly reduced and hence it would not be surprising to see differing submonolayer structures from those recorded by Kolaczkiewicz and Bauer for Gd [5]. This would be seen in an STM study of the growth, but to date only studies of the Gd/W(110) and Gd/W(100) systems have been published [26, 33]. Also changes in electronic structure being the cause of the reduced CLS of peak A are further ruled out by the similarity of the CLS for peak I.

## 4. Summary

From the data fitted only one interface peak is observed for each of the rare-earth/W(110) interfaces, indicating good ordering at the interfaces with no alloying. The interface is completed on deposition of 1.5–2.0 ML. At submonolayer coverages a contribution is seen from W atoms under the various submonolayer structures formed. This feature is attributed to several components, but these are not resolved in this study. The CLS found for the interface peak is similar for each of the three rare-earth metals, but differs for the submonolayer peak A. During deposition the surface peak is rapidly attenuated and its CLS decreases. The mechanism of the charge transfer leading to the shifts is still unclear. It is noted that the difference in evaporation temperature for Yb could give rise to the lower CLS observed for its submonolayer peak.

## Acknowledgments

## References

[1] Dowben P A, McIlroy D N and Li Dongqi 1996 *Surface Magnetism of the Rare Earth Metals, Handbook on the Physics and Chemistry of Rare Earths* vol 24, ed K A Gschneider and L Eyring (Amsterdam: North-Holland)
[2] Giergiel J, Pang A W, Hopster H, Guo X, Tong S Y and Weller D 1995 *Phys. Rev.* B **51** 10 201
[3] Quinn J, Li Y S, Jona F and Fort D 1992 *Phys. Rev.* B **46** 9694
[4] Weller D, Alvarado S F, Gudat K and Campagna M 1985 *Phys. Rev. Lett.* **54** 1555
[5] Kolaczkiewicz J and Bauer E 1986 *Surf. Sci.* **175** 487
[6] Duc T M, Guillot C, Lassailly Y, Lecante J, Jugnet Y and Verdine J C 1979 *Phys. Rev. Lett.* **43** 789
[7] Riffe D M, Wertheim G K and Citrin P H 1989 *Phys. Rev. Lett.* **63** 1976
[8] Riffe D M, Kim B, Erskine J L and Shinn N D 1994 *Phys. Rev.* B **50** 14 481
[9] Spanjaard D, Guillot C, Desjonquères M C, Tréglia G and Lecante J 1985 *Surf. Sci. Rep.* **5** 1–86
[10] Håkansson K L, Johansson H I P and Johannson L I 1994 *Phys. Rev.* B **49** 2035
[11] Alnot P, Auerbach D J, Behm J, Brundle C R and Viescas A 1989 *Surf. Sci.* **213** 1
[12] Jupille J, Purcell K G and King D A 1996 *Surf. Sci.* **367** 149
[13] Mullins D R and Lyman P F 1993 *Surf. Sci.* **285** L473
[14] Gerken F, Barth J, Kammerer R, Johansson L I and Flödström A 1982 *Surf. Sci.* **117** 468
   Kammerer R, Barth J, Gerken F, Flödström A and Johansson L I 1982 *Solid State Commun.* **41** 435
[15] Navas E, Starke K, Laubschat C, Weschke E and Kaindl G 1993 *Phys. Rev.* B **48** 14 753
   Fedorov A V, Laubschat C, Starke K, Weschke E, Barholz K-U and Kaindl G 1993 *Phys. Rev. Lett.* **70** 1719
   Fedorov A V, Arenholz E, Starke K, Navas E, Baumgarten L, Laubschat C and Kaindl G 1994 *Phys. Rev. Lett.* **73** 601
[16] Ortega J E, Himpsel F J, Li Dongqi and Dowben P A 1994 *Solid State Commun.* **91** 807
[17] White R G, Blyth R I R, Tucker N P, Lee M H and Barrett S D 1995 *J. Synchrotron Radiat.* **2** 261
[18] Doniach S and Sunjic M 1970 *J. Phys. C: Solid State Phys.* **3** 285
[19] Dhanak V R, Robinson A W, van der Laan G and Thornton G 1992 *Rev. Sci. Instrum.* **63** 1342
[20] Dowben P A, LaGraffe D and Onellion M 1989 *J. Phys.: Condens. Matter* **1** 6571
[21] Tucker N P, Blyth R I R, White R G, Lee M H, Robinson A W and Barrett S D 1995 *J. Synchrotron Radiat.* **2** 252
[22] Woodruff D P and Delchar T A 1994 *Modern Techniques of Surface Science* 2nd edn (Cambridge: Cambridge University Press) p 107
[23] Powell C J 1974 *Surf. Sci.* **44** 29
[24] Tucker N P, Blyth R I R, White R G, Lee M H and Barrett S D in preparation
[25] Zhang J, Dowben P A, Li Dongqi and Onellion M 1995 *Surf. Sci.* **329** 177
[26] Tober E D, Ynzunza R X, Westphal C and Fadley C S 1996 *Phys. Rev.* B **53** 5444
[27] Gaspar P, Eguiluz A G, Tsuei K D and Plummer E W 1991 *Phys. Rev. Lett.* **67** 2854
[28] Woratschek B, Sesselmann W, Kuppers J, Ertle G and Hamberland H 1985 *Phys. Rev. Lett.* **55** 1231
[29] Lamble G M, Brooks R S, King D A and Norman D 1988 *Phys. Rev. Lett.* **61** 1112
[30] Riffe D M, Wertheim G K and Citrin P H 1990 *Phys. Rev. Lett.* **64** 571
[31] Kolaczkiewicz J and Bauer E 1992 *Surf. Sci.* **265** 39
[32] Kolaczkiewicz J and Bauer E 1992 *Surf. Sci.* **273** 109
[33] White R G, Lee M H, Tucker N P, Barrett S D and Murray P W 1997 *Phys. Rev.* B **56** R10 071
[34] Hennig D, Methfessel M and Scheffler M 1994 *Surf. Sci.* **307–309** 933
   Methfessel M, Hennig D and Scheffler M 1995 *Surf. Rev. Lett.* **2** 197